

Eszter Barthazy* and Raphael Schefold

Institute for Atmospheric and Climate Science, ETH, 8093 Zürich Switzerland

1 INTRODUCTION

The properties of snowflakes such as their size distribution, fall velocity, axial ratio or their orientation when falling are important in modelling precipitation processes or in interpreting returned radar power, especially of polarized radar. The Institute of Atmospheric and Climate Science at the ETH has developed a ground-based optical spectrometer for the measurement of hydrometeors. The instrument works with two light beams which are vertically slightly offset. Thus, two images are recorded of each particle which can be used to calculate, in addition to the other properties, the exact fall velocity of the snowflakes. Hydrometeors can be recorded in the size range of 0.15 mm to 76 mm which includes also the very large snowflakes falling within or close to the melting layer without truncating their image.

2 HARDWARE

The instrument consists of three units: a sensor, an interface unit, and a standard PC.

The sensor A light source is producing a beam of uniform light directed towards an electronic line scan camera. The optical path of the beam is shielded by a rectangular tube except for a gap of 108.5 mm length near the light source. Precipitation particles falling through the light beam in this gap cast a shadow which is measured by the line scan camera. The camera is sensitive in two horizontal planes having a vertical distance of 9.45 (± 0.55) mm. The length of these measuring planes is given by the dimension of the gap of the housing, the width is given by the dimension of the line scan sensors in the camera and was determined to be 76.75 (± 4.25) mm. A top and a side view of the sensor unit is shown in Fig. 1.

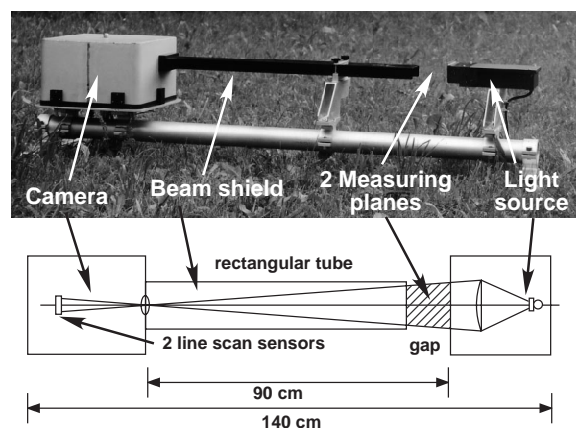


Fig. 1: Side and top view of the sensor unit.

* Corresponding author's address: Institute for Atmospheric and Climate Science, ETH Henggerberg HPP, CH-8093 Zürich, e-mail: eszter@atmos.umnw.ethz.ch

The camera also contains the electronic circuits necessary to drive the line scan sensors, to digitize the analog video signals, and to drive the lines to the interface unit. The CCD line scan sensors are monolithic integrated circuits containing a line of 512 photosensitive elements and two analog shift registers. The size of an element is 14 μm by 14 μm . The video information is read out serially with the two analog shift registers, one for the odd and one for the even numbered picture elements. The line scan frequency is 9470 Hz. Because there are two line scan sensors, four streams of analog video are generated. Each stream of video is passed through a comparator using a fixed threshold. Depending on whether the threshold is exceeded or not the corresponding picture element is considered to be bright or dark and the comparator puts out a digital one or zero.

The interface unit The interface unit converts the four serial video signals into 16 bit parallel words suitable as input for the PCI adaptor board of the PC.

The data acquisition The PC is a highspeed standard unit with direct access to the PCI bus via a standard PCI adaptor board to accommodate the high data rate of the optical disdrometer. The data acquisition begins to record the data as soon as a hydrometeor is passing one of the two horizontal planes of the light beam. The recording is stopped, when no hydrometeor has passed for a certain time. Such a record is called a block. A typical block is shown in Fig. 2. During precipitation such blocks are recorded repeatedly.

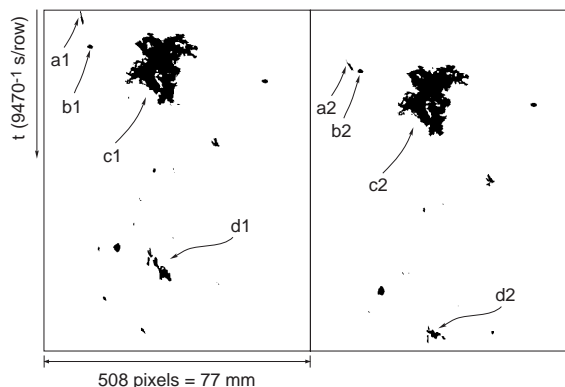


Fig. 2: A block containing all particles passing through the upper (left frame) and lower (right frame) sheet of light.

3 SOFTWARE

The optical spectrometer uses two horizontal planes of the lightbeam. The images of the measured hydrometeors are thus recorded in blocks with two sides, as shown in Fig. 2. To calculate the vertical fallspeed and other parameters of hydrometeors, two corresponding

images of hydrometeors have to be matched. Difficulties to match two images are given through three reasons:

- i. The vertical fallspeed of snowflakes is not only a function of their size (Locatelli and Hobbs, 1974, hereafter referred to as LH), as it is the case for raindrops. The time difference to pass the distance between the two light beams is thus undetermined (the small particle a is faster than the bigger particle c in Fig. 2). This leads to unknown vertical distances between the two images.
- ii. Horizontal winds lead to a shift of the horizontal position of the hydrometeor and thus of the images.
- iii. Hydrometeors can change their visible shape (e.g. due to rotation (particle d)).

A program (*Flocki*, an *igraph* under Wit from Logical Vision) overcomes these difficulties and calculates matches on the basis of different characteristics of the images. For a particle represented through matched images the horizontal shift v_h due to winds, vertical speed v_v and the dimensions of the particle, e.g. actual width w and height h are computed. The height h of the particle is proportional to $H \cdot v_v$, where H is the height of the image, simply because slower particles are longer within the light beam than faster particles.

Algorithm For each image inside a block, shape describing characteristics are calculated. These are height H , width W , number of pixels N , grayscale $G = H \cdot W/N$ and circumference C . Images touching the border of a block are not used, because their characteristics do not comply attributes of real particles. For each of these characteristics a matrix, e.g. $H_{i,j}$, is created, where the entry (i,j) of that matrix is representing the quality of a match for the i -th image left with the j -th image right with $0 \leq H_{i,j} \leq 1$, where 1 means compliance. If an entry $H_{i,j}$ is smaller than a given cut-off value, the entry is set to zero, not allowing a match for the couple (i,j) .

Furthermore, there are position describing characteristics. A matrix X describes horizontal shifts, whereas Y describes fallspeeds. For each couple (i,j) the shifts along the x - and y -axis are stored in $X_{i,j}$ and $Y_{i,j}$. Cut-off values allow only entries, where the values are inside certain bands. Cases with negative fallspeeds or too big horizontal shifts are thus excluded. The remaining entries are then converted into values $0..1$, where 1 means well inside the allowed band, 0 outside.

A matrix Z , where $Z_{i,j}$ describes the general quality of a match for the i -th image left with the j -th image right is found by weighted multiplication of the entries of the single matrices:

$$Z_{i,j} := H_{i,j}^{1/e_H} \cdot W_{i,j}^{1/e_W} \cdot N_{i,j}^{1/e_N} \cdot G_{i,j}^{1/e_G} \cdot X_{i,j}^{1/e_X} \cdot Y_{i,j}^{1/e_Y},$$

where e_v are the inverse exponents to weight the characteristics. Larger numbers e_v result in a higher weight of the corresponding entry.

At most, one image per side can correspond with one image on the other side. Therefore, we have to find a non-ambiguous general assignment of the images from one side to the images on the other side. Suppose n images left, m images right with $n \leq m$. If we find in the $n \cdot m$ -matrix Z n entries where not two

entries are in the same column or in the same row and where the sum over all these entries is the largest sum possible then we have the best non-ambiguous general assignment. There are two possible options:

- i. For sparsely populated blocks every possible general assignment is evaluated. The complexity of this procedure is proportional to $m!/(m-n)!$. The procedure finds the best general assignment, but is very CPU-intensive.
- ii. For densely populated blocks the general assignment is generated by choosing as first assignment the highest entry in Z and as second assignment the second highest entry which is not in the same row or in the same column like the highest entry. The third assignment is found by choosing the third highest entry which is not in the same row or column as the first or second chosen assignment. This procedure is repeated until no row or column is left. This option does not necessarily find the best general assignment, because of its assumptions (e.g. choosing the highest entry as first), but is fast.

Flocki returns the quality of the general assignment of the block (the sum over all entries belonging to the general assignment) together with properties of matched images within the block. The matched images represent hydrometeors. The calculated properties of the hydrometeors can be used for further case evaluation, as shown in section 4.

Discussion and Outlook The new algorithm works very well, if the images of one side of the block have differing shape describing characteristics. This is the case e.g. for big snowflakes. Uncertain fallspeeds require a wide band in y -direction. The weights belonging to the shape describing characteristics are then set higher than the weights belonging to the position describing characteristics. The differing shape describing characteristics ensure a good general assignment.

On the other hand, the images of small raindrops and graupel particles originate similar images. The shape describing characteristics can not produce a good general assignment as it is the case before. The quality of a good general assignment is now depending on a good choice of the allowed bands in x - and y -direction. For the case of no horizontal wind the allowed band in x -direction can be set very small. For particles with a roughly known size-fallspeed-correlation (const. density) the width of the allowed band in y -direction can be set depending on the size of the particle. Either one of these cases is necessary to compute a good general assignment.

4 CASE STUDIES

During the SOP of MAP (Mesoscale Alpine Programme) measurements of snow were made in the Alps of Northern Italy on Monte Moro (2800 m ASL). On 30 October 1999 a seven hour episode of snowfall was measured. Ice crystals were mainly of irregular type, some were of the broad branched stellar type. Ice crystals were unrimed and small unrimed aggregates were observed.

Fall velocity Fig. 3 shows the fall velocity of these snowflakes. There is a wide scatter of the fall velocities. On one hand, this can be attributed to the natural variability of the fall velocity of snow. On the other hand,

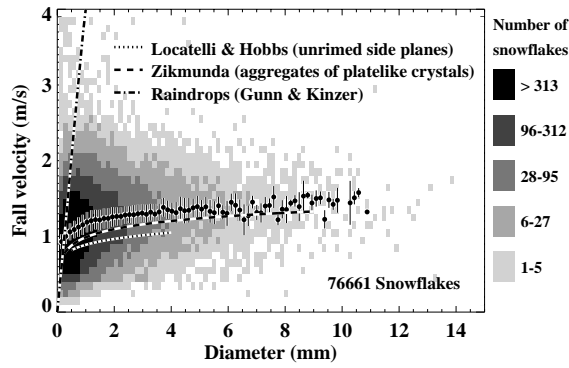


Fig. 3: Observed fall velocities of unrimed snowflakes at 720 mb.

this is also a result of the uncertainty of measuring the "size" of a snowflake. The "size" of a snowflake is determined by Flocki as the largest horizontal extension perpendicular to the light beams. This may not be the overall largest horizontal extension of the snowflake. Furthermore, it is not at all clear which dimension of a snowflake is suited best to act as a "size". Different authors use different approaches, e.g. the diameter of an equi-area circle as seen from above (LH). For each size class, the average fall velocity (dot) and the standard deviation (bar) has been calculated. The averages can be fitted with a power law of the form $v(D) = 1.16 \cdot D^{0.095}$ ($r^2 = 0.77$) for all sizes, or with $v(D) = 1.16 \cdot D^{0.101}$ ($r^2 = 0.94$) for particles smaller than 6 mm. As a comparison, fall velocity relationships from different authors are printed in Fig. 3. The relationship of Zikmunda (1972) for aggregates of platelike crystals compares very well to our observations, whereas the relationship of LH for aggregates of unrimed side planes shows smaller fall velocities. Here, it has to be remembered that we observe mainly irregular crystals with some broad branched stellars which probably compare better to the observations of the crystal types of Zikmunda than of LH.

Fig. 3 also shows that the average fall velocity is almost constant for the large snowflakes. The scatter introduced to the data by the underestimation of the largest extension of a snowflake must thus be small. Therefore, the scatter of fall velocities is mainly based on the natural variability of snowflake fall velocity.

Axis ratio In Fig. 4 the axis ratio of the snowflakes is shown. The average axis ratio of all sizes of snowflakes is below 1.0 which indicates oblate snowflakes. The scatter is again large, especially for the small particles. Firstly, scatter is due to natural variations of the axis ratio of the snowflakes of a given size. Secondly, scatter is introduced by the fact that the size of the snowflake, as measured by the instrument, is not necessarily its largest horizontal extension. Thus, the axis ratio may be overestimated. In contrast to the influence on the fall velocity, this may have a larger influence on the axial ratio.

Mixed phase precipitation On 15 March 1998, an interesting case was recorded where graupel particles were mixed with unrimed crystals and unrimed large aggregates. The duration of the episode was only about 10 minutes and mixing happened when a convective cell moved in with graupel particles overtaking

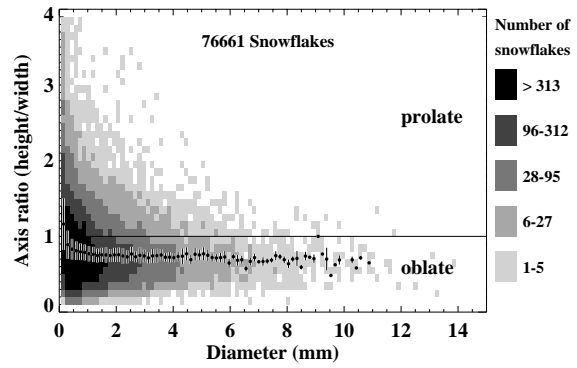


Fig. 4: Axis ratio of unrimed snowflakes.

the slowly falling unrimed ice particles. The fall velocity of the hydrometeors from this episode is shown in Fig. 5. The two phases can be distinguished clearly. As a comparison, fall velocity relations of graupel and of aggregates of unrimed side planes are shown from LH. This short episode shows the potential of the instrument to study mixed phases such as graupel and snowflakes or raindrops and snowflakes.

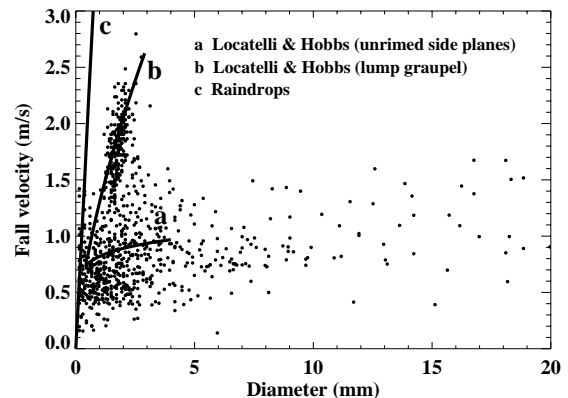


Fig. 5: Fall velocities of hydrometeors of a mixed phase episode with graupel and unrimed aggregates.

5 CONCLUSION

A large data set of observations of different precipitation types measured with the optical spectrometer has proven the field-worthiness of the instrument. First results obtained with the evaluation software have also shown that the matching of two images of hydrometeors, especially of snowflakes recorded with two vertically offset cameras is possible. Thus, new parameters of hydrometeors, such as their fall velocity and axial ratio are now available which could be measured up to now only for some selected snowflakes but not for a whole precipitation event.

6 REFERENCES

- Locatelli, J. D., and P. V. Hobbs, 1974. Fall speeds and masses of solid precipitation particles. *J. Geophys. Res.*, **79**, 2185–2197.
- Zikmunda, J., 1972. Fall velocities of spatial crystals and aggregates. *J. Atmos. Sci.*, **29**, 1511–1515.